JOURNAL OF APPLIED ELECTROCHEMISTRY 21 (1991) 760–766

Theoretical and experimental studies of current distribution in gas-evolving electrochemical reactors with parallel-plate electrodes

J. M. BISANG

Programa de Electroquímica Aplicada e Ingeniería Electroquímica (PRELINE), Facultad de Ingeniería Química, Universidad Nacional del Litoral, Santiago del Estero 2829, 3000 Santa Fe, Argentina

Received 2 February 1991; revised 5 March 1991

The current density distributions for a gas evolving electrochemical reactor with parallel-plate electrodes at different total currents were measured and calculated. The current density profiles were determined using a segmented electrode method. The numerically computed curves, according to a one-dimensional model, and the experimental measurements show good agreement. Furthermore, a comparison between several mathematical models is made.

Nomenclature

A	cross-sectional area (cm^2)
b	constant in the Tafel equation (V^{-1})
B	constant defined by Equation 20
C	constant defined by Equation 23 ($\Omega cm^2 V^{-2}$)
D	constant defined by Equation 24 (Ω)
e	electrode thickness (cm)
E	proportionality constant in Equation 27 ($cm^3 A^{-1} s^{-1}$)
F	Faraday constant ($A s mol^{-1}$)
G	volumetric gas flow rate ($cm^3 s^{-1}$)
i	current density ($A cm^{-2}$)
i_0	exchange current density ($A cm^{-2}$)
I	total current (A)
L	electrode length (cm)
N	number of experimental values in Equation 18
N_{Mac}	MacMullin number
P	gas pressure (atm)
Q	volumetric liquid flow rate ($cm^3 s^{-1}$)
R	gas constant ($atm\,cm^3 K^{-1} mol^{-1}$)
S	interelectrode distance (cm)
S_i	i electrode-to-membrane gap (cm)
S_D	separator thickness (cm)
T	temperature (K)
U_0	reversible cell voltage (V)
v	velocity ($cm s^{-1}$)
v^0	superficial flow velocity ($cm s^{-1}$)
v_s	single bubble rise velocity ($cm s^{-1}$)
v_{sw}	bubble swarm rise velocity ($cm s^{-1}$)
V	applied voltage to the reactor (V)
W	electrode width (cm)
y	axial coordinate (cm)

Greek characters

$\bar{\delta}_r$	mean relative deviation
$\Delta\phi_i$	ohmic drop in the anode-to-cathode gap (V)
$\Delta\phi_m$	ohmic drop in the metal phase (V)
ε	gas voidage
ε_m	limiting gas voidage
η	overvoltage (V)
ν_e	charge number of the electrode reaction
ρ^0	electrolyte resistivity (Ωcm)
ρ	resistivity (Ωcm)
σ	slip ratio

Subscripts

a	anodic
c	cathodic
D	separator
exp	experimental
th	theoretical
g	gas phase
m	metal phase
s	solution phase

1. Introduction

During the last few years gas generation in electrochemical systems has received considerable attention. Gas evolution has, at the same time, deleterious or beneficial effects on the performance of the reactor. Generally, one beneficial effect is the improvement of the mass and heat transfer conditions to the electrode surface due to turbulence enhancement by the gas-bubbles. Another beneficial aspect is the circulation of electrolyte through gas-lift. The deleterious effects of gas evolution are less in the electrode area due to the shielding effect, and the increase in effective resistivity in the gas-filled electrolyte, which in turn produces an increase in the resistive voltage losses and the resultant non-uniform current distribution in the reactor. This may affect the life of membranes and catalyst coatings. The last aspect will be treated here.

0021-891X/91 $03.00 + .12

The calculation of the current density distribution in a reactor requires the knowledge of the gas voidage as a function of the position in the electrolyte. The gas voidage can be expressed by the following equation

$$\varepsilon = \frac{A_g}{A} \tag{1}$$

Introducing the volumetric flow rate, $G = v_g A_g$, and rearranging yields

$$\varepsilon = \frac{v_g^0}{v_g} \tag{2}$$

Therefore, to calculate the gas voidage it is necessary to know the gas velocity at each point in the reactor. This requires the solution of a two-phase flow problem which may be solved from different points of view. Funk and Thorpe [1] define the slip ratio, σ, as the quotient between the velocities of the gas and liquid phases. Thus, Equation 1 can be expressed as

$$\varepsilon = \frac{1}{1 + Q\sigma/G} \tag{3}$$

In general, the slip ratio, σ, depends on the physical, physicochemical and geometrical parameters and there are several models which express the void fraction-slip ratio relationship. The simplest model is the homogeneous model in which σ is taken to be unity. In this case the velocity of gas bubbles relative to that of the solution is neglected. Nishiki [2] has recently dealt with the current distribution in a vertical cell assuming a homogeneous model.

Another approach to the problem of the gas voidage has been made by Nicklin [3], who demonstrated that the bubble rise velocity depends on the superficial gas and liquid velocities and also on the rise velocity of the bubble swarm, v_{sw}. He derived the following equation

$$\varepsilon = \frac{1}{1 + (Q + v_{sw}A)/G} \tag{4}$$

The Nicklin model is reduced to the homogeneous model when $v_{sw} = 0$, which is true for large gas voidage. The rise velocity of a bubble swarm is a function of both the gas voidage and the single bubble rise velocity, v_s. There are several equations to calculate v_{sw} which are summarized in [4]. Taking into account the Richardson-Zaki equation for v_{sw} and Equation 4, Rousar [5] and Rousar *et al.* [6] have modelled monopolar and bipolar electrolyzers.

However, the experimental results show that the gas voidage approaches a maximum when the volumetric gas flow rate increases but, contrary to the Nicklin equation, this maximum does not converge to 1. The experimental maximum value of the void fraction, ε_m, is substantially smaller than unity. Taking into account the limiting voidage, Kreysa and Kuhn [4] have proposed the coalescence barrier model, which can be represented as

$$\varepsilon = \left[\frac{1}{\varepsilon_m} + \frac{Q(1 - \varepsilon/\varepsilon_m)}{G(1 - \varepsilon)} + \frac{v_{sw}}{v_g^0}\right]^{-1} \tag{5}$$

Likewise, with the same purpose but making different considerations, Vogt [7] has derived a modified voidage equation as

$$\varepsilon = \left\{1 + \left[\left(\frac{1}{\varepsilon_m} - 1\right)^2 + \left(\frac{Q}{G}\right)^2\right]^{0.5} + \frac{v_{sw}}{v_g^0}\right\}^{-1} \tag{6}$$

For stationary electrolyte ($Q = 0$), Equation 5 coincides with Equation 6 and these Equations are equal to Equation 4 when the limiting voidage is 1.

Based on the coalescence barrier model, Martin and Wragg [8] have recently proposed a one-dimensional numerical model to describe gas void fraction and current distribution for different configurations of gas-evolving cells with stationary electrolyte. They have also included in their model the resistances of both electrodes and the over-potentials.

The present paper deals with the current distribution in gas-evolving electrochemical reactors with parallel-plate electrodes. The mathematical model presented here is one similar to that of Martin and Wragg [8] and the experimental values of current densities were determined using a reactor with a segmented counter electrode. The aim of this work is to compare the theoretical and experimental results in order to determine the validity and reliability of the model.

2. Mathematical model

The overall voltage balance for a parallel plate electrochemical reactor at the axial position y may be written as

$$V = U_0(y) + \Delta\phi_{m,a}(y) + \eta_a(y) + \Delta\phi_i(y) + \eta_c(y) + \Delta\phi_{m,c}(y) \text{ for all } y \tag{7}$$

In the following theoretical analysis some simplifying assumptions are made:

(i) The reversible cell voltage is not a function of y, which is a fair approach because in the Nernst equation large changes in the concentrations are necessary to cause an appreciable variation in U_0;

(ii) the ohmic drop in the metal phase of the anode is neglected due to the special construction of the reactor used in this work;

(iii) the thickness of the cathode is small with respect to distances in which significant potential variation takes place in the metal phase so that a one-dimensional model is applicable to calculate the potential distribution in the cathode;

(iv) in the solution phase the current flows unidirectionally, therefore each portion of the anode takes current from the cathode portion directly opposite to it. In a previous paper [9] this restriction was suppressed, however only a slight improvement in the prediction of the experimental results was obtained at the expense of more computation time;

(v) for each compartment, anodic or cathodic, and at the axial position y, the bubble distribution is uniform

along both the width and the thickness of the compartment, so that the gas voidage varies only in the y direction. This condition is imposed by the derivation of the electrolyte resistivity equations;

(vi) the reactor is isothermal.

With the first two assumptions, Equation 7 becomes:

$$\eta_a(y) + \Delta\phi_i(y) + \eta_c(y) + \Delta\phi_{m,c}(y) = \text{constant(1)} \quad (8)$$

The term $\Delta\phi_i(y)$ in Equation 8 is the sum of the ohmic drops in the gas-filled solution phases of the anodic and cathodic compartments and the ohmic drop in the separator between them; thus taking into account Ohm's law, $\Delta\phi_i(y)$ is given by

$$\Delta\phi_i(y) = [\rho_a(y)S_a + \rho_D S_D + \rho_c(y)S_c]i(y) \quad (9)$$

The effective electrolyte resistivity may be expressed by the Bruggeman equation

$$\rho/\rho^0 = (1 - \varepsilon)^{-3/2} \quad (10)$$

Introducing Equation 10 for each compartment into Equation 9 and rearranging yields.

$$\Delta\phi_i(y) = \{[1 - \varepsilon_a(y)]^{-3/2}S_a + N_{Mac}S_D + [1 - \varepsilon_c(y)]^{-3/2}S_c\}\rho^0 i(y) \quad (11)$$

where N_{Mac} is the MacMullin number [10] for the diaphragm and is defined as the ratio of the specific resistivity of the diaphragm filled with a given electrolyte relative to the electrolyte resistivity, ρ^0.

The ohmic drop in the metal phase of the cathode at the position y is given by

$$\Delta\phi_{m,c}(y) = \frac{\rho_m I}{We}y - \frac{\rho_m}{e}\int_0^y\int_0^y i(y)\,dy\,dy \quad (12)$$

obtained by the integration of the potential equation [11, 12] in the metal phase.

Introducing Equations 11 and 12 into Equation 8, using the Tafel equation for the electrode kinetics and rearranging yields

$$\{[1 - \varepsilon_a(y)]^{-3/2}S_a + N_{Mac}S_D + [1 - \varepsilon_c(y)]^{-3/2}S_c\} \times \rho^0 i(y) + \frac{\rho_m I}{We}y - \frac{\rho_m}{e}\int_0^y\int_0^y i(y)\,dy\,dy + \left(\frac{1}{b_a} + \frac{1}{b_c}\right)\ln i(y) = \text{constant(2)} \quad (13)$$

where the constant(2) is determined by solving Equation 13 at $y = 0$, thus

$$\text{constant(2)} = (S_a + N_{Mac}S_D + S_c)\rho^0 i(0) + \left(\frac{1}{b_a} + \frac{1}{b_c}\right)\ln i(0) \quad (14)$$

and the total current I is given by

$$I = W\int_0^L i(y)\,dy \quad (15)$$

Furthermore, the Kreysa and Kuhn expression (Equation 5) is used to describe the gas voidage in each compartment as a function of the position and the gas velocity referred to the cross-section of the compartment, $v^0_{g,i}$, is given by

$$v^0_{g,i} = \frac{RT}{Pv_{e,i}FS_i}\int_0^y i(y)\,dy \quad (16)$$

with $i = a$ or c.

The Richardson-Zaki equation is adopted to calculate the rise velocity of the bubble swarm, i.e.

$$v_{sw} = v_s(1 - \varepsilon)^{4.5} \quad (17)$$

The equations to calculate the gas voidage and the rise velocity of the bubble swarm will be discussed in more detail in item 5.

The current density distributions were obtained by iterative solution of Equations 13 to 15 simultaneously with Equations 5, 16 and 17 for each compartment. The solution of this system of equations was carried out numerically.

3. Experimental details

All experiments were performed in an electrochemical reactor with vertical parallel plate electrodes, as shown schematically in Fig. 1. The current density distribution was determined employing the segmented electrode method; and hydrogen- and oxygen-evolution from 1 M NaOH solution were the cathodic and anodic reactions respectively.

The reactor was made of acrylic material with both electrodes of nickel, 200 mm width and 600 mm long, arranged in a filterpress configuration.

The cathode, a sheet of 0.5 mm thick, was electrically

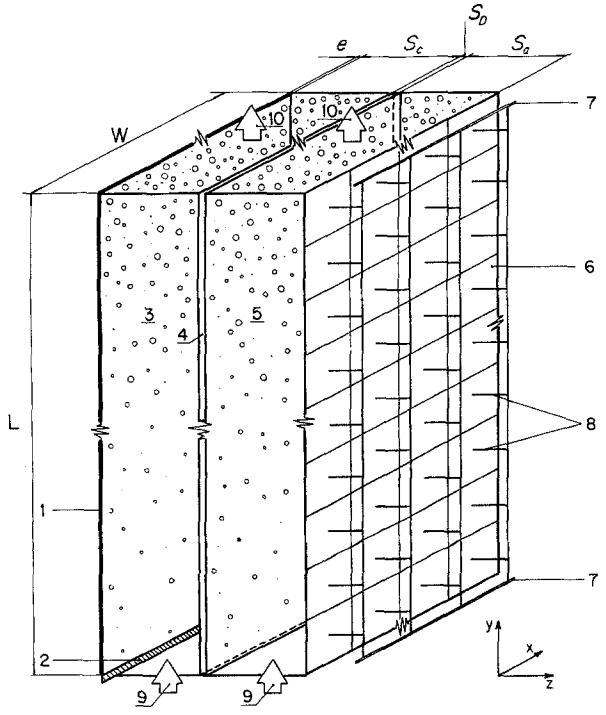

Fig. 1. Schematic representation of the reactor. (1) cathode, (2) cathodic current feeder, (3) cathodic compartment, (4) separator, (5) anodic compartment, (6) segmented anode, (7) anodic current feeder, (8) resistors, (9) electrolyte inlets; and (10) gas-electrolyte outlets.

fed along its lower edge. The cathode potential, in the feeder region, was measured against a Hg/HgO reference electrode in the same electrolyte solution. Special attention was paid to the construction and location of the Luggin-Haber tip, so as to ensure small ohmic drops in solution.

The anode was made of 192 squares, 24 mm side and 1 mm thick, arranged in 8 columns of 24 elements. The squares were insulated from one another by an approximately 1 mm thickness of epoxy resin. A calibrated resistor made from constantan wire, 100 mm long, 1.5 mm diameter and approximately 0.02 Ω resistance, was intercalated between the backside of each square and the current feeder of the anode. The current distribution was determined by measuring the ohmic drop in the corresponding resistor. The data acquisition was performed with an analogue multiplexer commanded by a computer. To represent more exactly the experimental reactor an additional term for voltage drop in the resistor should be introduced into Equation 7. However, in the mathematical modelling the voltage drop in the resistor was neglected with respect to the other terms of Equation 7 due to the small value of its resistance.

The anodic and cathodic compartments were separated by a diaphragm of asbestos cloth 2 mm thick and the electrode-to-separator gaps were 13 mm.

In order to achieve more uniform flow conditions along the electrodes, flow distributor plates with numerous small holes were arranged in the inlet of the electrolyte and in the outlet of the gas-electrolyte dispersions. The reactor was made part of a flow circuit system consisting of a reservoir, a pump, a flowmeter and two gas-liquid separators, with an overall electrolyte volume of 30 dm^3. The total volumetric liquid flow rate was 112 $cm^3 s^{-1}$ and approximately one half of the electrolyte flows through anodic compartment and the second half through cathodic compartment, which can be admitted due to the symmetrical construction of both compartments. The temperature was 31.5 ± 1.5° C.

4. Results and discussion

Figure 2 shows the current density as a function of the position for the eight columns of segmented electrode. It can be seen that the experimental points, for a given value of y, have a relative error, with respect to the mean value, of approximately ± 5%. These discrepancies between the current distributions for each column can be attributed to the lack of total uniformity in the flow conditions into the reactor in spite of the utilization of flow distributors. In the following paragraphs the current distributions correspond to the mean value of the eight columns.

It can be observed that at the inlet and outlet regions the current densities are lower than the expected values. The nature of this behaviour is unclear but I suspect it can be attributed to the effect of the change of flow area on the hydrodynamic flow conditions in the inlet region [13], which can alter the remotion of the bubbles from the electrode surface, and to the formation of small gas pockets in the outlet region.

In Fig. 3, comparisons between the experimentally determined current density distributions and the numerically calculated ones are made for several values of the total current. There is a close agreement between experimental and theoretical results. For the calculations of the theoretical curves, the rise velocities of single bubbles for hydrogen and oxygen have been taken from literature [4], therefore these data are only approximate. However the influence of this value on the shape of the current distribution function is not great; for example, a variation of 100% in v_s causes only a change of 5% in $i(0)$, which is the more sensitive point of the distribution. Due to the fact that the accurate experimental measurement of the limiting gas voidage is difficult, in this work ε_m for hydrogen and oxygen were obtained by fitting the experimental current density distribution of the experiment at low total current. When the current is low, and consequently the current densities at each electrode are also small, the terms for ohmic drop in the metal phase and

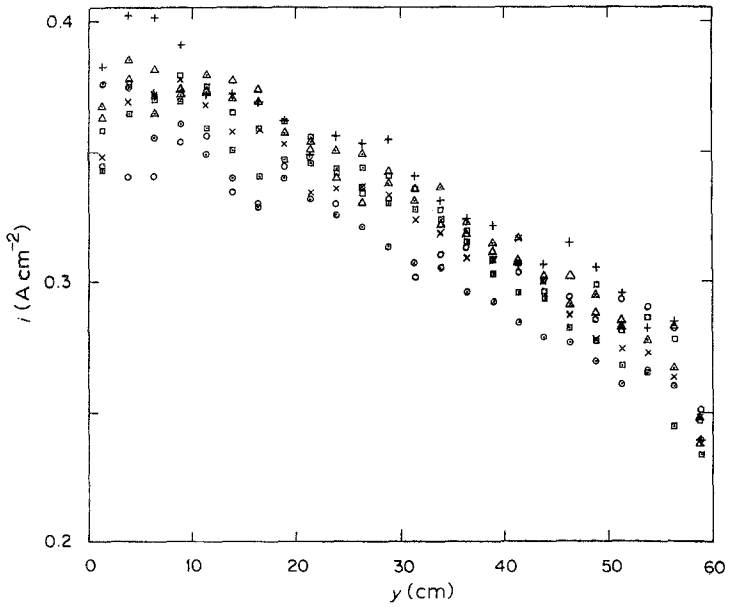

Fig. 2. Experimental current densities as a function of the position for the different columns. (⊙) column 1, (×) column 2, (⊡) column 3, (△) column 4, (△) column 5, (□) column 6, (+) column 7, (○) column 8. The external columns are the 1 and the 8. I = 389.21 A.

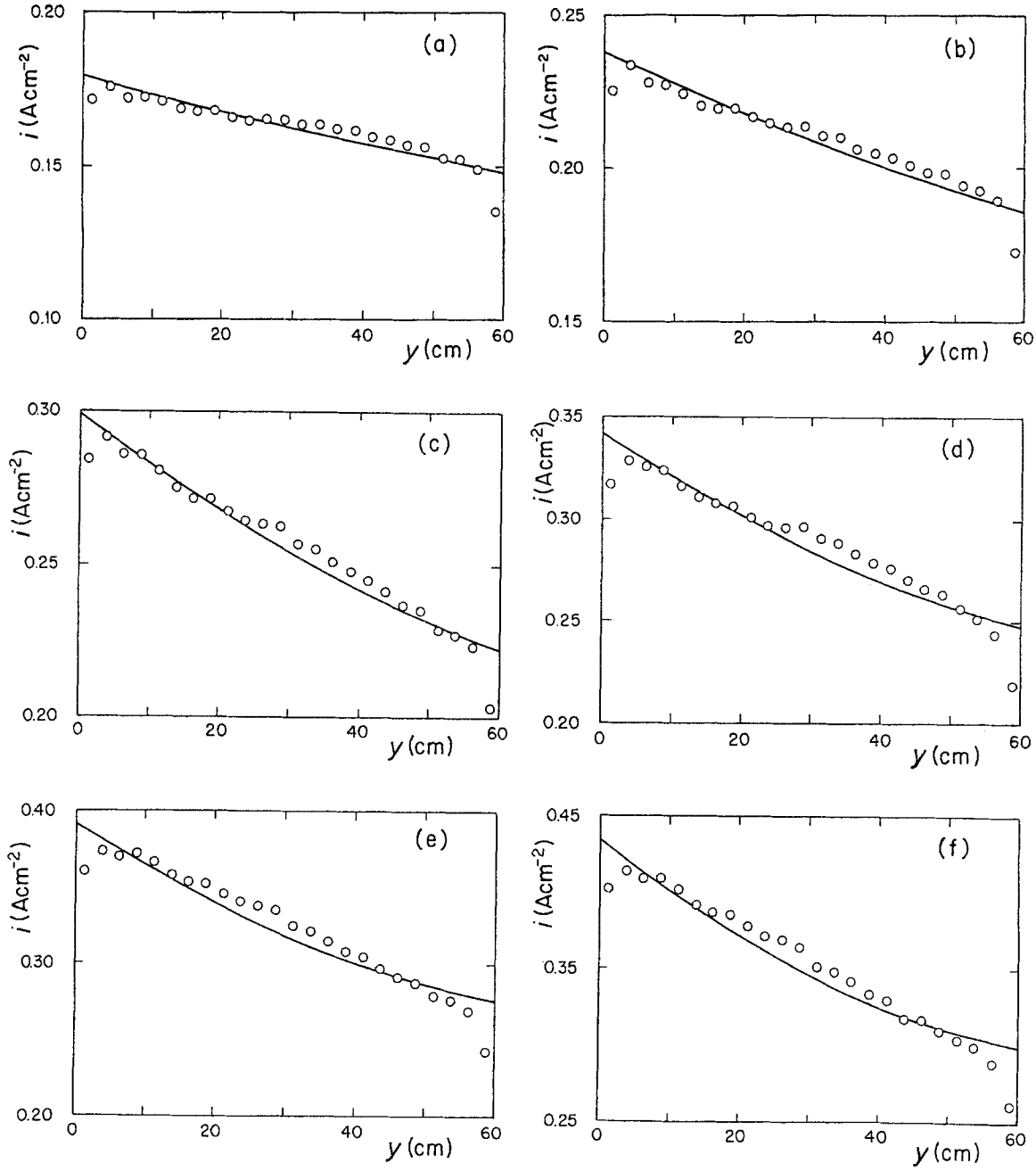

Fig. 3. Experimental and theoretical (——) current distributions. (a) 195.02, (b) 251.85, (c) 307.97, (d) 345.88, (e) 389.21 and (f) 424.07 A.

the overpotentials in Equation 8 can be neglected. Thus the model can be reduced to a simplified model, which considers only the ohmic drop in the anode-to-cathode gap. Therefore in order to obtain the limiting gas voidages, the experimental current densities at low total current were correlated by the least square method adjusting them to the simplified model.

Table 1 shows the obtained limiting gas voidages as well as the other fixed parameters used in modelling. The values of ε_m are higher than those reported by Kreysa and Kuhn [4] for more concentrated alkaline solutions and therefore it is confirmed that the

Table 1. Values of parameters used in modelling

ρ^0	5.56 Ω cm	L	60 cm
$\varepsilon_{m,a}$	0.26	W	20 cm
$\varepsilon_{m,c}$	0.38	e	0.05 cm
$v_{s,a}$	4.5 cm s^{-1}	S_a	1.3 cm
$v_{s,c}$	3.5 cm s^{-1}	S_c	1.3 cm
		S_D	0.2 cm
Q	112 cm^3 s^{-1}	b_a	22.99 V^{-1}
Q_a	0.5Q	b_c	25.58 V^{-1}
Q_c	0.5Q	$v_{e,a}$	4
ρ_m	7.41 × 10^{-6} Ω cm	$v_{e,c}$	2
N_{mac}	2		

Table 2. Review of the results

Fig. no.	*Curve*	*I (A)*	$\delta_r \times 10^2$
3	a	195.02	1.69
	b	251.85	1.65
	c	307.97	1.60
	d	345.88	2.34
	e	389.21	2.65
	f	424.07	2.68

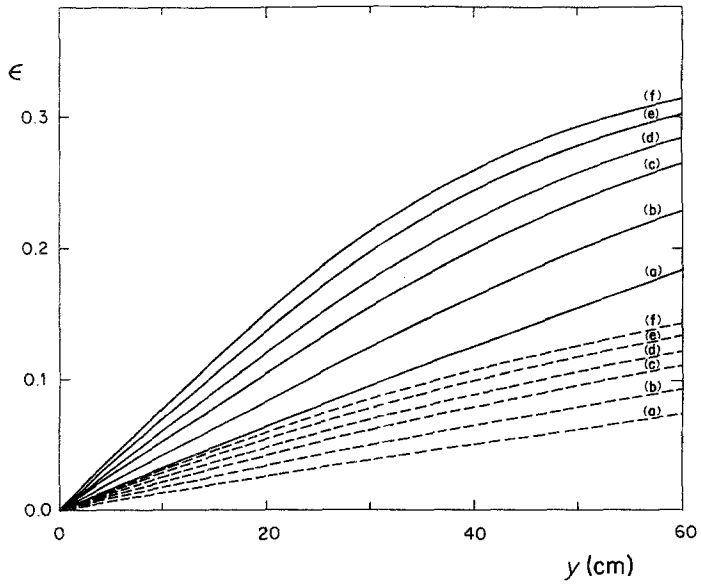

Fig. 4. Gas voidage as a function of the position for different total currents corresponding to the current distribution curves of Fig. 3. Full line (——): catholyte. Dashed line (– – –): anolyte. Parameters according to Table 1.

limiting voidage decreases with increasing electrolyte concentration.

Table 2 summarizes the results. In column 4, the mean relative deviation $\bar{\delta}_r$, defined as:

$$\bar{\delta}_r = \frac{1}{N}\sum_{i=1}^{N}\frac{|i_{exp}(y_i) - i_{th}(y_i)|}{i_{th}(y_i)}, \qquad (18)$$

is given. It must be noted that $\bar{\delta}_r$ is in all cases lower than 3% showing that the mathematical treatment is reliable for the modelling of these electrochemical systems.

Figure 4 depicts the calculated gas voidage as a function of the position for each compartment at different total currents. The curves show that in no case was limiting behaviour achieved.

5. Comparisons of models

The six terms on the right hand side in Equation 7 are functions of the axial position y but their sum is constant and each presents a different function with y. Therefore some terms in Equation 7 can be neglected with respect to others and thus various models are possible:

I. A first simple case is to take into account only ohmic drop in and overpotential of the electrode, which is the extension to parallel-plate electrodes of the model reported in [11] and the following current density distribution equation can be derived:

$$i(y) = i_0 \exp[b\eta(0)]\left\{\frac{\cos(B)}{\cos[B(1 - y/L)]}\right\}^2 \qquad (19)$$

whereas the constant B is given by the implicit formula

$$B = L\left\{\frac{\rho_m b}{2e} i_0 \exp[b\eta(0)]\right\}^{1/2}\cos(B) \qquad (20)$$

II. A more complex situation is achieved by adding to the further model the ohmic drop term in the solution phase but it is considered homogeneous and isotropic and the current flows unidirectionally, which is the generalization to parallel-plate reactors of the model developed in [14]. In this case the current distribution can be obtained by numerical solution of the set of equations:

$$A[\eta(y)]\frac{d^2\eta(y)}{dy^2} + C\left[\frac{d\eta(y)}{dy}\right]^2 - D = 0 \qquad (21)$$

where

$$A[\eta(y)] = \frac{\exp[-b\eta(y)]}{i_0} + \rho^0 Sb \qquad (22)$$

$$C = \rho^0 Sb^2 \qquad (23)$$

$$D = \rho_m/e \qquad (24)$$

with boundary conditions

$$y = 0 \quad \eta(y) = \eta(0) \qquad (25)$$

$$y = 0 \quad \frac{d\eta(y)}{dy} = \frac{-\rho_m I}{\{1 + \rho^0 Sbi_0 \exp[b\eta(0)]\}\, We} \qquad (26)$$

where I is given by Equation 15.

III. Considering only one solution phase and the gas voidage-superficial gas velocity relationship expressed by Equation 3, the current density distribution is given by

$$i(y) = \frac{2Q\sigma}{5EWL}\left[\left(\frac{IE}{\sigma Q} + 1\right)^{5/2} - 1\right] \times \left\{\left[\left(\frac{IE}{\sigma Q} + 1\right)^{5/2} - 1\right]\frac{y}{L} + 1\right\}^{-3/5} \qquad (27)$$

where E is the volume of gas evolved per unit of charge. When the slip ratio is unity, Equation 27 yields the current distribution according to the homogeneous model [2].

IV. The simplified Rousar model. Taking into account all the terms in the voltage balance equation for electrolyzers with a small electrode height, small current density and high rate of flow electrolyte, where the local current density does not differ appreciably from the average one, Rousar *et al.* [6] derived analytically

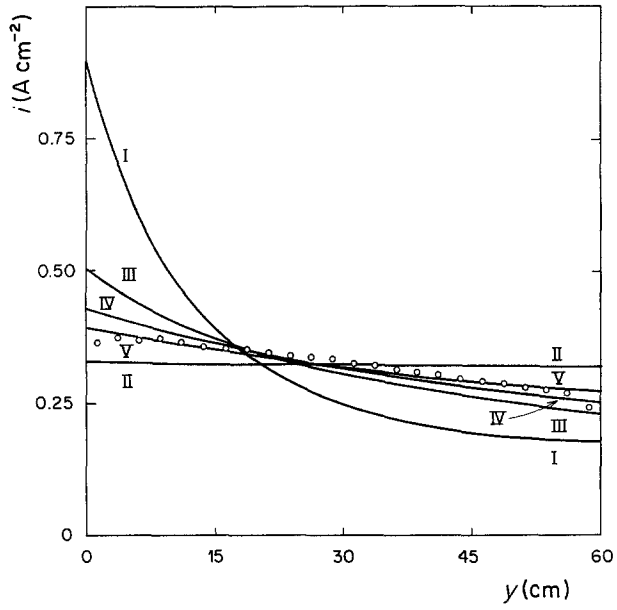

Fig. 5. Current distributions according to different models. I: Equation 19. II. In accordance with Equation 21. III. Equation 27. IV: Simplified Rousar *et al.* model (Equation 53 in [6]). V: model reported here. The experimental results correspond to curve (e) of Figure 3. I = 389.21 A.

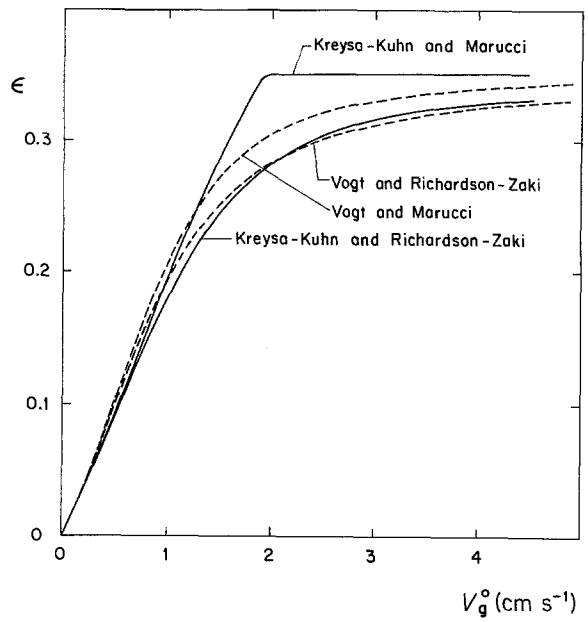

Fig. 6. Gas voidage as a function of superficial gas velocity. ε_m = 0.35, v_s = 3.5 cm s^{-1}, Q = 112 cm^3 s^{-1}, A = 52 cm^2.

an equation (Equation 53 in [6]) for the current distribution.

In Fig. 5, comparisons between the current distributions in accordance with the models I, II, III, IV and the model reported here are made. The experimental points correspond to curve (e) of Fig. 3. In general all curves have the same shape, however the model reported here gives the best agreement with the experimental results. It can be also observed that the current densities distribution according to the simplified Rousar model is close to the experimental one. The agreement between them is better when the total current is lower. Likewise, at low total current the simplified Rousar model and the model reported here give the same result.

The model developed under 2 can also be solved taking into account the Vogt expression, Equation 6, and describing the motion of the bubbles using the Marucci relationship with the modification suggested by Kreysa [15]:

$$v_{sw} = v_s \frac{(1 - \varepsilon/\varepsilon_m)^2}{1 - (\varepsilon/\varepsilon_m)^{5/3}} \qquad (28)$$

In Fig. 6 the gas voidage is plotted as a function of the superficial gas velocity according to the four possible combinations between Equations 5 and 6 with Equations 17 and 28. It was observed that the use of the Richardson-Zaki equation reduces the computation time. Figure 6 shows that the different pairs of equations agree satisfactorily at low and high values of velocity but the curves differ in the middle range of velocities. However, this behaviour is irrelevant from a practical viewpoint because the maximal discrepancy in the computed gas voidage with regard to the mean value is approximately $\pm 11\%$, which produces an error of only $\pm 7\%$ for the calculations of the current densities and this error is tolerable for engineering purposes.

6. Conclusion

The agreement between the theoretical current distributions and the experimental results is close, therefore the reported mathematical model should be recognized as a helpful tool to design electrochemical reactors with gas-evolving electrodes.

Acknowledgements

The author would like to thank Stiftung Volkswagenwerk and Deutscher Akademischer Austauschdienst (DAAD) of the Federal Republic of Germany for donating scientific equipment and Consejo Nacional de Investigaciones Científicas y Técnicas (CONICET), Argentina for financial support of this work.

References

[1] J. E. Funk and J. F. Thorpe, *J. Electrochem. Soc.* **116** (1969) 48.
[2] Y. Nishiki, K. Aoki, K. Tokuda and H. Matsuda, *J. Appl. Electrochem.* **16** (1986) 615.
[3] D. J. Nicklin, *Chem. Eng. Sci.* **17** (1962) 693.
[4] G. Kreysa and M. Kuhn, *J. Appl. Electrochem.* **15** (1985) 517.
[5] I. Rousar, *J. Electrochem. Soc.* **116** (1969) 676.
[6] I. Rousar, V. Cezner and J. Hostomsky, *Collect. Czech. Chem. Commun.* **36** (1971) 1.
[7] H. Vogt, *J. Appl. Electrochem.* **17** (1987) 419.
[8] A. D. Martin and A. A. Wragg, *ibid.* **19** (1989) 657.
[9] J. M. Bisang, *ibid.* **20** (1990) 723.
[10] J. Van Zee, R. E. White and A. T. Watson, *J. Electrochem. Soc.* **133** (1986) 501.
[11] J. M. Bisang and G. Kreysa, *J. Appl. Electrochem.* **18** (1988) 422.
[12] J. M. Bisang, *Lat. Am. Appl. Res.* **18** (1988) 63.
[13] D. J. Pickett and C. J. Wilson, *Electrochim. Acta* **27** (1982) 591.
[14] J. M. Bisang, *J. Appl. Electrochem.* **19** (1989) 500.
[15] G. Kreysa, *Ber. Bunsenges. Physik. Chem.* **92** (1999) 1194.